Germanium-antimony-selenium-tellurium thin films: Clusters formation by laser ablation and comparison with clusters from mixtures of elements

Fei Huang, Tomas Halenkovic, Marion Baillieul, Virginie Nazabal, Petr Nemec, Josef Havel

Germanium-antimony-selenium-tellurium Thin Films: Clusters Formation by Laser Ablation and Comparison with Clusters from Mixtures of Elements.

Fei Huang,[1] Tomáš Halenkovič,[2] Marion Baillieul,[2] Virginie Nazabal,[2,3] Petr Němec,[2] and Josef Havel[1*]

[1]Department of Chemistry, Faculty of Science, Masaryk University, Kamenice 5/A14, 62500 Brno, Czech Republic

[2]Department of Graphic Arts and Photophysics, Faculty of Chemical Technology, University of Pardubice, Studentská 573, 53210 Pardubice, Czech Republic

[3]Univ Rennes, CNRS, ISCR UMR6226, ScanMAT UMS 2001, F-35000 Rennes, France

*Author to whom correspondence should be addressed. Email: havel@chemi.muni.cz

Phone: +420 549494114, Fax: +420 549492494

Abstract

Quaternary Ge-Sb-Se-Te thin films deposited from $Ge_{19.4}Sb_{16.7}Se_{63.9-x}Te_x$ (x=5, 10, 15, 20) glass-ceramics targets by rf magnetron sputtering were studied using laser ablation quadrupole ion trap time of flight mass spectrometry. Binary, ternary, and quaternary $Ge_aSb_bSe_cTe_d$ clusters were formed and their stoichiometry was determined. By comparison of the clusters obtained from quaternary Ge-Sb-Se-Te thin films and those from ternary Ge-

Sb-Te materials, we found that Ge-Te species are not detected from the quaternary system. Furthermore, Ge-Se and Se-Te species are missing in mass spectra generated from Ge-Sb-Se-Te thin films. From the Ge-Sb-Se-Te thin films, 16 clusters were detected while ternary Ge-Sb-Se glasses yielded 26 species. This might be considered as a signal of higher stability of Ge-Sb-Se-Te thin films which is increasing with a higher content of Te. The missing (Se_2^+, Ge_aSb^+ (a = 1-4), and $GeSe_c^+$ (c = 1, 2)) and new (Ge^+ and Sb_bTe^+ (b = 1-3)) clusters may indicate that some of the structural features of the films ($Ge_2Se_{6/2}$ and $Se_2Sb\text{-}SbSe_2$) were replaced by ($GeSe_{4-x}Te_x$ and $SbSe_{3-x}Te_x$) ones. In addition, when comparing the stoichiometry of clusters formed from Ge-Sb-Se-Te thin films with those from the mixtures of the elements, only Sb_3^+ and $SbSe^+$ were observed in both cases. The knowledge gained concerning clusters stoichiometry contributes to the elucidation of the processes proceeding during plasma formation used for the chalcogenide thin films deposition.

KEYWORDS

Ge-Sb-Se-Te, amorphous chalcogenides, thin films, magnetron sputtering, laser ablation, clusters, mass spectrometry

1 | INTRODUCTION

Chalcogenide glasses and amorphous thin films are widely used[1-4] because of their unique advantages of broad transmission window in IR spectral region, high refractive index, and photosensitivity to light exposure.[5-9] Moreover, chalcogenide glasses exhibit huge Kerr nonlinearities at a femtosecond time scale which can reach values of several orders of

magnitude larger than that of silica glass, variable two-photon absorption depending on their bandgap, and insignificant free carrier absorption.[10] Given the above-mentioned properties, the application of chalcogenide glasses in all-optical signal processing based on nonlinear effects for telecommunication systems has been studied.[2]

Ternary Ge-Sb-Se glasses are important members of the chalcogenide group of glasses; their physicochemical properties have been intensively studied.[8, 11-14] Furthermore, Ge-Sb-Se amorphous thin films fabricated using different physical vapor deposition techniques are in the center of interest of several research groups.[15-19]

The attention of some authors has been already attracted by modifying of Ge-Sb-Se glasses by tellurium. The substitution of selenium by heavier tellurium atoms may lead to the decrease of phonon energies which may result in a broadening of IR transparency. Besides that, the increasing tellurium concentration may cause the increase of the (non)linear refractive index which can make Ge-Sb-Se-Te glasses and thin films promising materials for nonlinear optical applications. In fact, the quaternary Ge-Sb-Se-Te system was studied from the point of view of glass-forming ability,[20] structure,[21] thermal properties,[22] optical, and other properties.[23-24] Finally, thin films from the Ge-Sb-Se-Te quaternary system might be considered as a promising alternative to Ge-Sb-Te layers in phase-change memory applications as proposed recently by Wang[25] and Zhang.[26]

It has been shown that exposure of amorphous chalcogenides (in both bulk and thin film forms) with a pulsed laser, having high enough pulse energy density, leads to laser ablation (LA). The plasma plume, which is formed due to laser ablation, contains many clusters which can be detected by time-of-flight mass spectrometry (TOFMS). Indeed, this technique can be used to elucidate the composition of the structural fragments present in the plasma generated

during the interaction of high energy laser pulses with chalcogenide glasses[27] or amorphous thin films.[28]

The aim of this paper is to evaluate the changes in amorphous Ge-Sb-Se-Te thin films when Se is partially replaced by Te by studying the chemistry of clusters formed by LA. In parallel, the comparison of the stoichiometry's of clusters detected by laser ablation of thin films with those of the species generated via laser ablation synthesis (LAS) from binary, ternary, and quaternary mixtures of the elements (i. e. Ge-Sb, Ge-Te, Sb-Te, Se-Te, and Ge-Sb-Se-Te) was performed.

2 | EXPERIMENTAL PROCEDURE

2.1 | Chemicals

Acetonitrile and (germanium, antimony, selenium, and tellurium of 99.999% purity) were purchased from Sigma-Aldrich (Steinheim, Germany). A quartz apparatus from Heraeus Quarzschmelze (Hanau, Germany) was used to produce ultrapure double distilled water. All the other reagents were of analytical-grade purity.

2.2 | Thin films fabrication and characterization

Glass-ceramics $Ge_{19.4}Sb_{16.7}Se_{63.9-x}Te_x$ (x=5, 10, 15, 20) sputtering targets, whose basic composition ($Ge_{19.4}Sb_{16.7}Se_{63.9}$) corresponds to $(GeSe_2)_{70}(Sb_2Se_3)_{30}$ identified earlier (from the point of view of its nonlinear optical properties and photostability) as promising glass composition in $(GeSe_2)_{100-x}(Sb_2Se_3)_x$ pseudobinary system,[8] were fabricated by a conventional melt-quenching technique as described elsewhere.[29] Thin films with thickness in the 780-840 nm range were deposited at room temperature by rf (13.56 MHz) magnetron

sputtering onto single crystalline silicon <100> substrates employing the MPE600 multi-chamber deposition system (Plassys-Bestek, France). The deposition conditions varied in terms of electrical power applied on targets (10 or 15 W) and argon pressures (0.5 or 1 Pa).

The chemical composition of thin films was determined through energy-dispersive X-ray analysis (EDS) connected with a scanning electron microscope (JSM 6400-OXFORD Link INCA, JEOL Ltd., Japan). The amorphous state of the layers was confirmed by the X-ray diffraction measurements.

2.3 | Sample preparation for mass spectrometry

Germanium, antimony, selenium, and tellurium were separately crushed into powder using an agate mortar and then suspended in acetonitrile (1 mg/ml). From the suspensions, 1 μL sample was deposited on a target and dried. When the thin films were analyzed, a narrow piece of parafilm was used to fix the Ge-Sb-Se-Te thin films on the target.

2.4 | Mass spectrometry

Mass spectra were recorded using either an AXIMA CFR or AXIMA Resonance mass spectrometer, both from Kratos Analytical Ltd (Manchester, UK), in both positive and negative ion modes. Both instruments were coupled with a time-of-flight detection and equipped with a nitrogen laser (337 nm). The AXIMA Resonance was equipped with a Quadruple Ion Trap. The laser repetition rate was set to 5 Hz with a pulse time width of 3 ns. Mass spectra were obtained by accumulating 1000 laser shots. The laser energy was scaled in arbitrary units (a.u.) from 0 to 180; this relative scale will be used hereafter. The irradiated spot size was approximately 150 μm in diameter. The maximum laser pulse energy was 250 μJ. The laser fluence was ~1 J/cm^2.

2.5 | Software and computation

The stoichiometry of clusters was determined via a comparison of theoretical and experimental isotopic envelopes using Launchpad software (Kompact version 2.9.3, 2011) from Kratos Analytical Ltd. (Manchester, UK).

3 | RESULTS

An overview of the thin films deposition parameters with resulting thin films chemical composition is given in Table 1. We note that there is good agreement between the nominal chemical composition of deposited thin films and corresponding sputtering targets.

The mass spectra were recorded in both positive and negative ion modes by using the reflectron mode. The formation of clusters generated from mixtures of elements and thin films via LA was studied. It was shown that in positive ion mode, mass spectra were of higher intensity compared to the negative ion mode and a higher number of species was observed. Therefore, the results presented here are for the positive ion mode. We note that LAS of antimony-selenium and germanium-selenium mixtures with different ratios have already been studied.[30-31]

3.1 | LAS of germanium-antimony clusters from Ge:Sb = 1:1, 1:10, and 10:1 mixtures

A comparison of mass spectra of germanium-antimony mixtures with different molar ratios is shown in Figure 1. For the ratio with a high excess of antimony, $GeSb_3^+$ was the only germanium-antimony cluster observed apart from Sb_b^+ (b = 2-4) species. In addition, low intensity Sb_bO^+ (b = 2, 3), $Sb_3O_4^+$, $Sb_4O_5^+$, and $Sb_5O_7^+$ clusters were also identified. For the 1:1 ratio of germanium to antimony, or for high content of Ge, there were many germanium-

antimony clusters detected such as $GeSb_b^+$ (b = 2-4), $Ge_2Sb_b^+$ (b = 1-3), $Ge_3Sb_b^+$ (b = 1-3), $Ge_4Sb_b^+$ (b = 1, 2), and Ge_6Sb^+ and also germanium unary species Ge_a^+ (a = 1-7) were found. A comparison of experimental and theoretical isotopic patterns demonstrating the overlap of $GeSb_4^+$ and Ge_6Sb^+ clusters is shown in Fig. S1. As seen in the figure, there is a good agreement between experimental and theoretical mass spectra.

3.2 | LAS of germanium-tellurium clusters from Ge:Te = 1:1, 1:10, and 10:1 mixtures

A comparison of mass spectra for germanium-tellurium mixtures in different ratios at the laser energy of 120 a.u. is shown in Fig. S2A. It can be seen that the spectra features are similar. The $GeTe_d^+$ (d = 2, 3) clusters are the germanium-tellurium species observed (in the mass spectrum of a mixture with large excess of Ge (Ge:Te = 10:1)). In addition to the Ge_4^+, Ge_5^+, Te_d^+ (d = 2-6), $GeTe_d^+$ (d = 2, 3), and $Ge_2Te_d^+$ (d = 2, 3) clusters, some oxidized Te_dO^+ (d = 2-4) and hydroxylated Te_dOH^+ (d = 2, 3) species were also generated. A good agreement of the theoretical isotopic pattern of the $GeTe_2^+$ cluster with the experimental pattern can be seen in Fig. S2B.

3.3 | LAS of antimony-tellurium clusters from Sb:Te = 1:1, 1:10, and 10:1 mixtures

Fig. S3A shows a comparison of mass spectra for antimony-tellurium mixtures at different ratios measured at the same laser energy (120 a.u.). It is shown that only for the ratio with high antimony concentrations, antimony-tellurium clusters like $SbTe_d^+$ (d = 1, 2), Sb_2Te^+, and Sb_3Te^+ were observed, while Te_d^+ (d = 2-6) species were observed in all spectra. In addition to the clusters mentioned, Sb_b^+ (b = 3-6) and oxidized Sb_bO^+ (b = 2, 3), $Sb_2O_2^+$, $Sb_3O_4^+$, and $Sb_3TeO_6^+$ species were also detected. A comparison of experimental and theoretical isotopic patterns for Sb_3Te^+ provided in Fig. S3B shows that they are in good agreement.

3.4 | LAS of selenium-tellurium clusters from Se:Te = 1:1, 1:10, and 10:1 mixtures

An example of LAS mass spectra for selenium-tellurium mixtures (concerning the generation of $Se_bTe_d^+$ clusters) is shown in Fig. S4A. For the ratio in which the tellurium was in high excess over selenium, the intensity of the spectra features was high. When the tellurium concentration was higher than or equal to selenium, Se_c^+ (c = 2-8), Te_d^+ (d = 2-5), Se_cTe^+ (c = 1-6), and $Se_cTe_2^+$ (c = 1, 3) clusters were observed. Even when the selenium was in high excess to tellurium, besides Se_c^+ (c = 2-8), only the $SeTe_4^+$ cluster was detected. The good agreement between the experimental and theoretical mass spectra related to the formation of $SeTe_4^+$ is shown in Fig. S4B.

3.5 | LAS of germanium-antimony-selenium-tellurium clusters from Ge:Sb:Se:Te = 1:1:1:1 mixtures

An example of mass spectra for the clusters generated from quaternary element mixture is shown in Figure 2. In addition to Sb_3^+, Te_2^+, Ge_3Sb^+, $Se_3Te_2^+$, Se_c^+ (c = 2-8), $SbSe_c^+$ (c = 1, 2, 5), and Se_cTe^+ (c = 3, 4, 6, 7) clusters, some low-intensity $Sb_3O_4^+$, $Sb_4O_{5\text{-}6}^+$, and $Sb_5O_7^+$ species were also observed. Arbitrary, signal corresponding Se_4Te^+ species was selected and it is shown in Fig. S5; the experimental and theoretical isotopic patterns for Se_4Te^+ cluster are in good agreement.

3.6 | LA TOF MS of Ge-Sb-Se-Te thin films with different Se:Te ratio

A comparison of LA TOFMS data of four selected thin films (Nr. 3, 7, 11, and 15) at the same laser energy (150 a.u.) is shown in Figure 3. It was observed that when tellurium is incorporated into thin films and its content increases, the stability of the thin film increases. This is deduced from the fact of decreased intensities of the spectra with the increased

content of tellurium. The clusters produced from the 16 quaternary Ge-Sb-Se-Te thin films are the same. In addition to the Ge^+, Sb^+, Sb_3^+, and binary Sb_bSe^+ (b = 1-3), $Sb_2Se_2^+$, $Sb_3Se_c^+$ (c = 2-4), Sb_bTe^+ (b = 1-3) clusters, ternary Sb_3SeTe^+, $Ge_4SbSe_4^+$, and quaternary $GeSb_2SeTe_2^+$ species were also observed. A comparison of experimental and theoretical isotopic patterns for the ternary Sb_3SeTe^+ cluster is given in Fig. S6, showing a good agreement of the experiment with the theoretical model. The clusters formed from quaternary Ge-Sb-Se-Te thin films are from more than 50% the same as the clusters detected from ternary Ge-Sb-Se glasses (nine Sb_b^+ (b = 1, 3), $SbSe^+$, $Sb_2Se_c^+$ (c = 1, 2), and $Sb_3Se_c^+$ (c = 1-4) species are identical).[27] Contrary, the clusters originating from quaternary Ge-Sb-Se-Te thin films were mostly different from those generated from the ternary Ge-Sb-Te system.[32] For example, only three species are common (Ge^+, Sb_2Te^+, and Sb_3Te^+).

4 | DISCUSSION

A review of the species identified in LA TOFMS data of mixtures of elements and those detected from thin films is provided in Table 2 and Table 3. When comparing the stoichiometry of the clusters generated from quaternary system Ge-Sb-Se-Te to those generated from ternary Ge-Sb-Te materials,[32] it was found that Ge-Te clusters are missing. This can be explained that Te was at least partially replaced by Se in the structure. It was also observed that no Ge-Se clusters were detected from the quaternary system. Probably it is because the bond energy Ge-Se is higher than Ge-Sb, Ge-Te, Se-Se, and Sb-Se (Ge-Se = 2.44 eV, Ge-Sb = 1.48 eV, Ge-Te = 1.87 eV, Se-Se = 2.14 eV, and Sb-Se = 2.25 eV).[33-34] While Se-Te clusters were not detected from the quaternary system, many of them were generated during LAS of the mixtures of elements. The missing Se-Te species is probably because that

the entity $SbSe_{3-x}Te_x$[35] is present in the structure (bond energy of Se-Te = 2.00 eV is higher than Sb-Te = 1.73 eV), so we observed not Se-Te but Sb-Te species. On the other hand, Sb-Se clusters were detected from Ge-Sb-Se-Te layers which demonstrate that Se is the most probably bonded to Sb in the structure of studied quaternary materials.

When comparing the stoichiometry of the clusters obtained from Ge-Sb-Se-Te thin films to those observed from ternary Ge-Sb-Se glasses,[27] it was found that

i) A lower number of clusters is formed. Furthermore, for tellurium doped thin films it is demonstrated that the formation of binary and ternary clusters is diminished. A review of the species (Ge-Sb, Ge-Se, Sb-Se, and Ge-Sb-Se) detected both in Ge-Sb-Se and Ge-Sb-Se-Te is given in Table 4. These indicate that the quaternary system shows greater stability than the ternary system;

ii) Sb_b^+ (b = 1, 3) and the most of Sb-Se clusters ($SbSe^+$, $Sb_2Se_c^+$ (c = 1, 2), and $Sb_3Se_c^+$ species (c = 1-4)) are the same. Comparing LAS of mixtures of elements, Sb-Se mixtures are the easiest ones to form clusters. Indeed, these bonds are high energy bonds, and once they are formed it is not easy to incorporate other elements especially when there have some lower energy bonds that coexist in the system;

iii) Se_2^+, Ge_aSb^+ (a = 1-4), and $GeSe_c^+$ (c = 1, 2) clusters are missing whereas Ge^+ and Sb_bTe^+ (b = 1-3) clusters were generated. The $SbSe_{3/2}$ pyramids, $GeSe_{4/2}$ tetrahedra, $Ge_2Se_{6/2}$ entities, and $Se_2Sb\text{-}SbSe_2$ species form the structure of Ge-Sb-Se glasses. From the point of view of chemical boding, homopolar Ge-Ge, Sb-Sb, and Se-Se bonds, as well as heteropolar Ge-Se and Sb-Se (perhaps also Ge-Sb) bonds, are present in the structure.[8] We suggest that $SbSe_{3/2}$ pyramidal and $GeSe_{4/2}$ tetrahedral are too stable (pyramidal, tetrahedral structure, and high bond energy of Sb-Se or Ge-Se bonds) to be decomposed by MS. A similar observation was observed for sulfides.[36] This probably means that the entities ($Ge_2Se_{6/2}$ and $Se_2Sb\text{-}SbSe_2$)

were replaced by the entities ($GeSe_{4-x}Te_x$ and $SbSe_{3-x}Te_x$),[35] and thus the reactions in the plasma plume changed. In addition, when comparing the stoichiometry of the clusters generated from Ge-Sb-Se-Te mixtures of elements with those generated from Ge-Sb-Se-Te thin films, only two clusters (Sb_3^+ and $SbSe^+$) are common. The Se_c^+ (c = 2-8) clusters were not observed in thin films. The bond energies of Ge-Se, Sb-Se, and Se-Te are higher than Ge-Sb, Ge-Te, and Sb-Te, which leads to the difficult decomposition of the Se-containing species.

5 | CONCLUSION

Laser ablation with quadrupole ion trap time of flight mass spectrometric analysis was used to characterize Ge-Sb-Se-Te thin films. The LAS of the clusters from the elements was found to be a suitable method to follow tellurium incorporation, i.e. the replacement of Se by Te in ternary Ge-Sb-Se system. It was demonstrated that the replacement of selenium with tellurium is causing that fewer clusters are produced which might indicate greater stability of the quaternary Ge-Sb-Se-Te thin films. Furthermore, it was observed that when the percentage of tellurium is increasing, the stability of the thin films increases. The species present in the plasma originating from quaternary Ge-Sb-Se-Te thin films were discussed. It was found that (Se_2^+ and Ge containing clusters Ge_aSb^+ (a = 1-4), and $GeSe_c^+$ (c = 1, 2) are missing), (Ge^+ and Sb_bTe^+ (b = 1-3) clusters are new), and (nine clusters (Sb_b^+ (b = 1, 3), $SbSe^+$, $Sb_2Se_c^+$ (c = 1, 2), and $Sb_3Se_c^+$ (c = 1-4)) are the same) when comparing the clusters to those generated from ternary Ge-Sb-Se glasses. These observations indicate some chemical/structural changes induced by Te incorporation. Besides, the comparison of quaternary Ge-Sb-Se-Te layers and ternary Ge-Sb-Te materials demonstrating the chemistry

changes was discussed. In addition, comparing the stoichiometry of clusters observed from Ge-Sb-Se-Te thin films with those from mixtures of its constituting elements was described. These results would enable a better understanding of the plasma processes for Ge-Sb-Se-Te thin films deposition as well as a description of structural motifs and chemical bonding in the plasma plume.

SUPPLEMENTARY INFORMATION

The supplementary information file contains mass spectra.

ACKNOWLEDGEMENTS

This work was funded with support from the Grant Agency of the Czech Republic (Project No. 19-24516S). The authors appreciate the financial support from the LM2018103 project funded by the Ministry of Education, Youth and Sports of the Czech Republic. F.H. is grateful for the financial support from Project no. MUNI/A/1390/2020 for the Analytical, Physical, and Chemical methods for Geological, Biological, and Synthetic Materials. Our appreciation goes to Dr. L. Prokes for his help with mass spectrometry measurements.

REFERENCES

1. Zakery A, Elliott SR. Optical properties and applications of chalcogenide glasses: a review. J. Non-Cryst. Solids. 2003;330:1-12.

2. Eggleton BJ, Luther-Davies B, Richardson K. Chalcogenide photonics. Nat. Photonics. 2011;5:141-148.

3. Adam JL, Zhang XH. (Eds.): Chalcogenide Glasses: Preparation, Properties and Application., Woodhead Publishing Series in Electronic and Optical Materials, Oxford 2014.

4. Wuttig M, Bhaskaran H, Taubner T. Phase-change materials for non-volatile photonic applications. Nat Photonics. 2017;11:465–476.

5. Lucas P, Yang Z, Fah MK, Luo T, Jiang S, Boussard-Pledel C, et al. Telluride glasses for far infrared photonic applications. Opt. Mater. Express. 2013;3:1049-1058.

6. Meneghini C, Villeneuve A. As_2S_3 photosensitivity by two-photon absorption: holographic gratings and self-written channel waveguides. J. Opt. Soc. Am. B. 1998;15:2946–2950.

7. Shimakawa K, Kolobov A, Elliott S. Photoinduced effects and metastability in amorphous semiconductors and insulators. Adv. Phys. 1995;44:475-588.

8. Olivier M, Tchahame J, Němec P, Chauvet M, Besse V, Cassagne C, et al. Structure, nonlinear properties, and photosensitivity of $(GeSe_2)_{100-x}(Sb_2Se_3)_x$ glasses. Opt. Mater. Express. 2014;4:525-540.

9. Calvez L, Yang Z, Lucas P. Light-induced matrix softening of Ge-As-Se network glasses. Phys. Rev. Lett. 2008;101:177402.

10. Sanghera J, Florea C, Shaw L, Pureza P, Nguyen V, Bashkansky M, et al. Non-linear properties of chalcogenide glasses and fibers. J. Non-Cryst. Solids. 2008;354:462-467.

11. Němec P, Olivier M, Baudet E, Kalendova A, Benda P, Nazabal V. Optical properties of $(GeSe_2)_{100-x}(Sb_2Se_3)x$ glasses in near-and middle-infrared spectral regions. Mater. Res. Bull. 2014;51:176-179.

12. Varshneya AK, Mauro DJ. Microhardness, indentation toughness, elasticity, plasticity, and brittleness of Ge–Sb–Se chalcogenide glasses. J. Non-Cryst. Solids. 2007;353:1291-1297.

13. Wei WH, Wang RP, Shen X, Fang L, Luther-Davies B. Correlation between Structural and Physical Properties in Ge–Sb–Se Glasses. J. Phys. Chem. C. 2013;117:16571-16576.

14. Giridhar A, Narasimham P, Mahadevan S. Density and microhardness of Ge-Sb-Se glasses. J. Non-Cryst. Solids. 1981;43:29-35.

15. Chen Y, Shen X, Wang RP, Wang GX, Dai SX, Xu TF, et al. Optical and structural properties of Ge–Sb–Se thin films fabricated by sputtering and thermal evaporation. J Alloys Comp. 2013;548:155-160.

16. Olivier M, Němec P, Boudebs G, Boidin R, Focsa C, Nazabal V. Photosensitivity of pulsed laser deposited Ge-Sb-Se thin films. Opt. Mater. Express. 2015;5:781-793.

17. Lin L, Wang GX, Shen X, Dai SX, Xu TF, Nie QH. Photo-induced structural changes in Ge-Sb-Se films. Infrared Phys Technol. 2017;81:59-63.

18. Halenkovič T, Gutwirth J, Kuriakose T, Bouška M, Chauvet M, Renversez G, et al. Linear and nonlinear optical properties of co-sputtered Ge-Sb-Se amorphous thin films. Opt. Lett. 2020;45:1523-1526.

19. Baudet E, Sergent M, Němec P, Cardinaud C, Rinnert E, Michel K, et al. Experimental design approach for deposition optimization of RF sputtered chalcogenide thin films devoted to environmental optical sensors. Sci. Rep. 2017;7:3500.

20. Bordas S, Casas-Vazquez J, Clavaguera N, Clavagura-Mora M. Glass-forming ability in the Ge-Sb-Te-Se quaternary system. Thermochim. Acta. 1979;28:387-393.

21. Fabian M, Svab E, Pamukchieva V, Szekeres A, Todorova K, Vogel S, et al. Reverse Monte Carlo modeling of the neutron and X-ray diffraction data for new chalcogenide Ge–Sb–S (Se)–Te glasses. J. Phys. Chem. Solids. 2013;74:1355-1362.

22. Svoboda R, Málek J. Thermal behavior of Se-rich $GeSb_2Se_{(4-y)}Te_y$ (glassy) system. J. Alloys Compd. 2016;670:222-228.

23. Yin N, Xu J, Chang F, Jian Z, Gao C. Effect of Te proportion on the properties of $Ge_{25}Sb_{10}Se_{65-x}Te_x$ chalcogenide glasses. Infrared Phys. Technol. 2019;96:361-365.

24. Sharma N, Sharda S, Katyal SC, Sharma V, Sharma P. Effect of Te on linear and non-linear optical properties of new quaternary Ge-Se-Sb-Te chalcogenide glasses. Electron. Mater. Lett. 2014;10:101–106.

25. Wang H, Guo TQ, Xue Y, Lv SL, Yao DN, Zhou ZG, et al. The phase change memory features high-temperature characteristic based on Ge-Sb-Se-Te alloys. Mater. Lett. 2019;254:182–185.

26. Zhang YF, B.Chou J, Li JY, Li HS, Du QY, Yadav A, et al. Broadband transparent optical phase change materials for high-performance nonvolatile photonics. Nat. Commun. 2019;10:4279.

27. Šútorová K, Prokeš L, Nazabal V, Bouška M, Havel J, Němec P. Laser Desorption Ionisation Time-of-Flight Mass Spectrometry of Chalcogenide Glasses from $(GeSe_2)_{100-x}(Sb_2Se_3)_x$ System. J. Am. Ceram. Soc. 2015,98:4107-4110.

28. Mawale R, Halenkovič T, Bouška M, Gutwirth J, Nazabal V, Bora PL, et al. Mass spectrometric investigation of amorphous Ga-Sb-Se thin films, Sci. Rep. 2019;9:10213.

29. Baudet E, Gutierrez-Arroyo A, Němec P. Bodiou L, Lemaitre J, De Sagazan O, et al. Selenide sputtered films development for MIR environmental sensor. Opt. Mater. Express. 2016;6:2616-2627.

30. Huang F, Prokeš L, Havel J. Laser ablation synthesis of antimony selenide clusters with simultaneous laser desorption ionization (LDI) quadrupole ion trap mass spectrometry. J. Am. Soc. Mass Spectrom. 2019;30:634–638.

31. Mawale R, Halenkovič T, Bouška M, Gutwirth J, Nazabal V, Takáts V, et al. Laser desorption ionization time-of-flight mass spectrometry of Ge_xSe_{1-x} chalcogenide glasses, their thin films, and Ge:Se mixtures. J. Non-Cryst. Solids. 2019;509:65-73.

32. Houška J, Peña-Méndez EM, Kolář J, Přikryl J, Pavlišta M, Frumar M, et al. Laser desorption time-of-flight mass spectrometry of atomic switch memory $Ge_2Sb_2Te_5$ bulk materials and its thin films. Rapid Commun. Mass Spectrom. 2014;28: 699-704**.**

33. Rao KJ, Mohan R. Chemical bond approach to determining conductivity band gaps in amorphous chalcogenides and pnictides. Solid State Commun. 1981;39:1065–1068.

34. Lee JH, Lee WH, Park JK, Yi JH, Shin SY, Park BJ, et al. Thermal properties of ternary Ge–Sb–Se chalcogenide glass for use in molded lens applications. J. Non-Cryst. Solids. 2016;431:41-46.

35. Abdellaoui N, Starecki F, Boussard-Pledel C, Shpotyuk Y, Doualan JL, Braud A, et al. Tb^{3+} doped $Ga_5Ge_{20}Sb_{10}Se_{65-x}Te_x$ (x = 0-37.5) chalcogenide glasses and fibers for MWIR and LWIR emissions. Opt. Mater. Express. 2018;8:2887-2900.

36. Huang F, Wágner T, Frumarová B, Fraenkl M, Koštál P, Havel J. Laser Desorption Ionization Time-of-Flight Mass Spectrometry of Silver-Doped $(GeS_2)_{50}(Sb_2S_3)_{50}$ Chalcogenide Glasses. ACS Omega. 2020;5:28965–28971.

Captions to the figures

FIGURE 1 Mass spectra from LAS of germanium-antimony mixtures with different molar ratios in the 250-650 *m/z* range. Conditions: positive ion mode; laser energy 120 a.u.

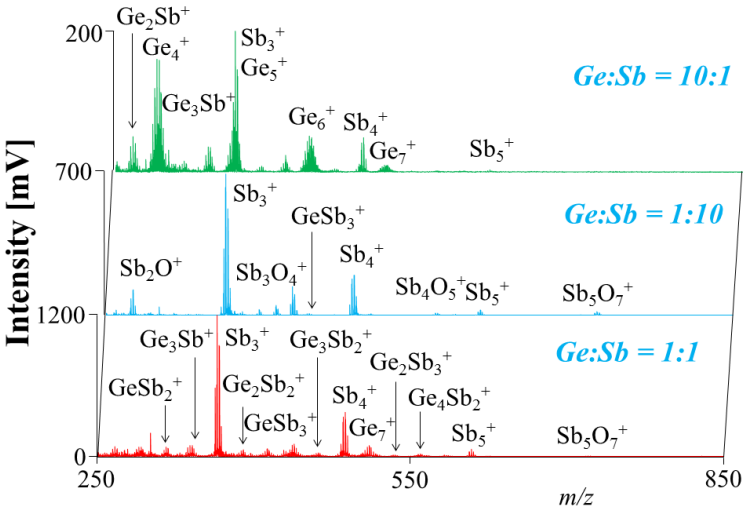

FIGURE 2 Mass spectra from LAS of germanium-antimony-selenium-tellurium mixtures with the molar ratio of 1:1:1:1 in the 150-750 *m/z* range. Conditions: positive ion mode; laser energy 120 a.u.

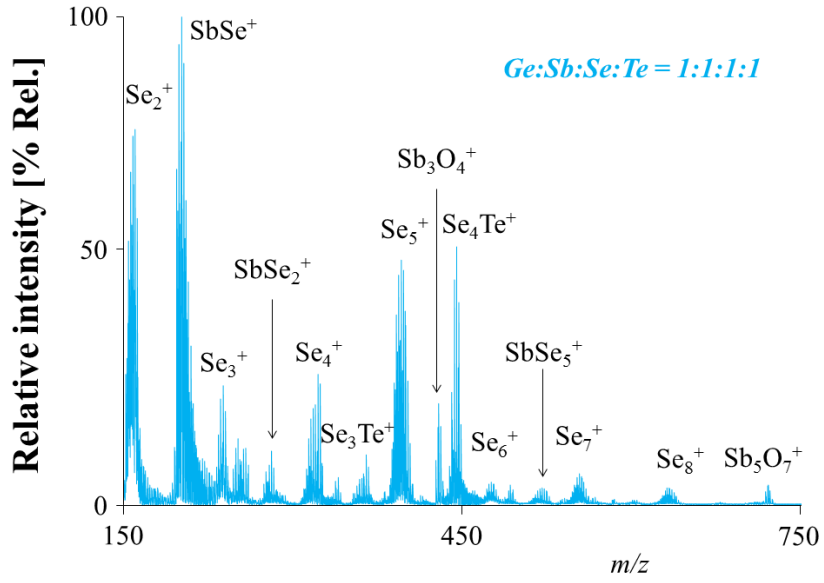

FIGURE 3 LA TOFMS data of Ge-Sb-Se-Te thin films in the 50-750 *m/z* range. Conditions: positive ion mode; laser energy 150 a.u.

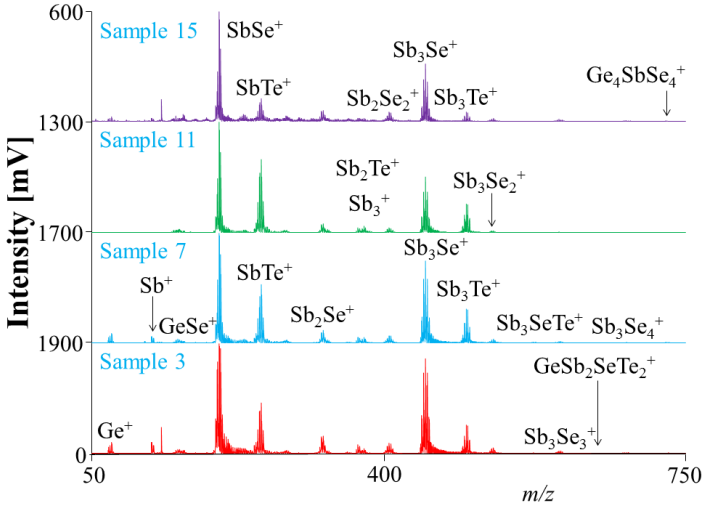

Film Nr.	Sputtering target	Power (W)	Ar pressure (Pa)	Composition (at. %)
1	$Ge_{19.4}Sb_{16.7}Se_{58.9}Te_5$	10	0.5	$Ge_{22.0}Sb_{16.9}Se_{54.6}Te_{6.5}$
2		10	1	$Ge_{19.5}Sb_{16.6}Se_{56.5}Te_{7.4}$
3		15	0.5	$Ge_{20.7}Sb_{17.3}Se_{55.0}Te_{6.9}$
4		15	1	$Ge_{19.3}Sb_{17.0}Se_{56.4}Te_{7.4}$
5	$Ge_{19.4}Sb_{16.7}Se_{53.9}Te_{10}$	10	0.5	$Ge_{21.7}Sb_{17.9}Se_{49.8}Te_{10.7}$
6		10	1	$Ge_{19.3}Sb_{17.4}Se_{51.2}Te_{12.1}$
7		15	0.5	$Ge_{20.5}Sb_{18.1}Se_{50.1}Te_{11.3}$
8		15	1	$Ge_{20.0}Sb_{17.7}Se_{50.9}Te_{11.4}$
9	$Ge_{19.4}Sb_{16.7}Se_{48.9}Te_{15}$	10	0.5	$Ge_{21.3}Sb_{18.1}Se_{45.6}Te_{15.0}$
10		10	1	$Ge_{19.9}Sb_{17.6}Se_{46.4}Te_{16.2}$
11		15	0.5	$Ge_{19.4}Sb_{19.1}Se_{45.0}Te_{16.6}$
12		15	1	$Ge_{19.1}Sb_{17.9}Se_{46.0}Te_{16.9}$
13	$Ge_{19.4}Sb_{16.7}Se_{43.9}Te_{20}$	10	0.5	$Ge_{19.1}Sb_{17.4}Se_{42.1}Te_{21.4}$
14		10	1	$Ge_{17.8}Sb_{19.8}Se_{39.8}Te_{22.7}$
15		15	0.5	$Ge_{18.7}Sb_{20.2}Se_{39.3}Te_{21.7}$
16		15	1	$Ge_{17.7}Sb_{19.7}Se_{40.0}Te_{22.6}$

Captions to the tables

TABLE 1 The summary of deposition parameters of Ge-Sb-Se-Te thin films. Chemical composition (±1 at. %) was determined by EDS.

TABLE 2 Clusters generated from mixtures of elements (the molar ratio of elements in binary mixture was 1:1, 1:10, and 10:1).

System	Clusters								References
Ge-Sb	Ge^+	Ge_2^+	Ge_3^+	Ge_4^+	Ge_5^+	Ge_6^+	Ge_7^+		This work
	Sb_2^+	Sb_3^+	Sb_4^+	Sb_5^+					
	$GeSb_2^+$	$GeSb_3^+$	$GeSb_4^+$						
	Ge_2Sb^+	$Ge_2Sb_2^+$	$Ge_2Sb_3^+$						
	Ge_3Sb^+	$Ge_3Sb_2^+$	$Ge_3Sb_3^+$						
	Ge_4Sb^+	$Ge_4Sb_2^+$							
	Ge_6Sb^+								
Ge-Te	Ge_4^+	Ge_5^+							This work
	Te_2^+	Te_3^+	Te_4^+	Te_5^+	Te_6^+				
	$GeTe_2^+$	$GeTe_3^+$							
	$Ge_2Te_2^+$	$Ge_2Te_3^+$							
Ge-Se	Ge_4^+								[31]
	Se_2^+	Se_3^+	Se_4^+	Se_5^+	Se_6^+	Se_7^+	Se_8^+		
	$GeSe_2^+$	$GeSe_3^+$	$GeSe_4^+$	$GeSe_5^+$	$GeSe_6^+$	$GeSe_7^+$	$GeSe_8^+$	$GeSe_2$	
	$Ge_2Se_4^+$	$Ge_2Se_6^+$							
	Ge_4Se^+	$Ge_4Se_2^+$	$Ge_4Se_3^+$	$Ge_4Se_4^+$					
	Ge_5Se^+	$Ge_5Se_2^+$	$Ge_5Se_3^+$	$Ge_5Se_5^+$					
Sb-Se	Se_4^+	Se_5^+	Se_6^+	Se_7^+	Se_8^+	Se_9^+			[30]
	$SbSe_2^+$	$SbSe_3^+$	$SbSe_4^+$	$SbSe_5^+$	$SbSe_6^+$	$SbSe_7^+$	$SbSe_8^+$		
	Sb_2Se^+	$Sb_2Se_2^+$	$Sb_2Se_3^+$	$Sb_2Se_4^+$	$Sb_2Se_5^+$	$Sb_2Se_6^+$			
	Sb_3Se^+	$Sb_3Se_2^+$	$Sb_3Se_3^+$	$Sb_3Se_4^+$	$Sb_3Se_5^+$				
	Sb_4Se^+	$Sb_4Se_2^+$	$Sb_4Se_3^+$						
	Sb_5Se^+	$Sb_5Se_2^+$							
Sb-Te	Sb_3^+	Sb_4^+	Sb_5^+	Sb_6^+					This work
	Te_2^+	Te_3^+	Te_4^+	Te_5^+	Te_6^+				
	$SbTe^+$	$SbTe_2^+$							
	Sb_2Te^+								
	Sb_3Te^+								
Se-Te	Se_2^+	Se_3^+	Se_4^+	Se_5^+	Se_6^+	Se_7^+	Se_8^+		This work
	Te_2^+	Te_3^+	Te_4^+	Te_5^+					
	$SeTe^+$	$SeTe_2^+$	$SeTe_4^+$						
	Se_2Te^+								
	Se_3Te^+	$Se_3Te_2^+$							
	Se_4Te^+								
	Se_5Te^+								
	Se_6Te^+								
Ge-Sb-Se-Te 1:1:1:1	Sb_3^+								This work
	Se_2^+	Se_3^+	Se_4^+	Se_5^+	Se_6^+	Se_7^+	Se_8^+		
	Te_2^+								
	Ge_3Sb^+								
	$SbSe^+$	$SbSe_2^+$	$SbSe_5^+$						
	$TeSe_3^+$	$TeSe_4^+$	$TeSe_6^+$	$TeSe_7^+$					

System	Clusters					References
Ge-Sb-Se	Se_2^+					[27]
	Sb^+	Sb_3^+				
	$GeSb_3^+$	$Ge_2Sb_3^+$	$Ge_3Sb_3^+$	$Ge_4Sb_3^+$		
	$GeSe^+$	$GeSe_2^+$				
	$SbSe^+$	$SbSe_2^+$				
	Sb_2Se^+	$Sb_2Se_2^+$	$Sb_2Se_3^+$	$Sb_2Se_4^+$		
	Sb_3Se^+	$Sb_3Se_2^+$	$Sb_3Se_3^+$	$Sb_3Se_4^+$	$Sb_3Se_5^+$	
	$GeSbSe_2^+$	$GeSb_4Se^+$	$GeSb_5Se^+$			
	$Ge_9Sb_2Se_5^+$	$Ge_9Sb_2Se_6^+$	$Ge_9Sb_2Se_7^+$			
Ge-Sb-Te	Ge^+	Ge_2^+				[32]
	Te_2^+	Te_3^+				
	$GeTe^+$	$GeTe_2^+$				
	$SbTe_2^+$					
	Sb_2Te^+	$Sb_2Te_3^+$				
	Sb_3Te^+					
	$GeSbTe_2^+$	$GeSbTe_3^+$				
Ge-Sb-Se-Te	Ge^+					This work
	Sb^+	Sb_3^+				
	$SbSe^+$					

	Sb_2Se^+	$Sb_2Se_2^+$		
	Sb_3Se^+	$Sb_3Se_2^+$	$Sb_3Se_3^+$	$Sb_3Se_4^+$
	$TeSb^+$	$TeSb_2^+$	$TeSb_3^+$	
	Sb_3SeTe^+			
	$Ge_4SbSe_4^+$			
	$GeSb_2SeTe_2^+$			

TABLE 3 Clusters generated from Ge-Sb-Se bulk glasses, Ge-Sb-Te thin layers/bulk glasses, and Ge-Sb-Se-Te thin films.

TABLE 4 The number of clusters observed from ternary Ge-Sb-Se glasses and from thin films analysed in this work.

	[27]	This work
Ge-Sb	4	0
Ge-Se	2	0
Sb-Se	11	7
Ge-Sb-Se	6	1